

Bir Konteyner Gemisi İçin Kapsamlı Yalpa Sönümü Değerlendirmesi ve Hareket Analizi

Ferdi Çakıcı¹, Rabia Yenilmez²

^{1,2}Yıldız Teknik Üniversitesi, Gemi İnşaatı ve Denizcilik Fakültesi , Gemi İnşaatı ve Gemi Makineleri Mühendisliği Bölümü, İstanbul, Türkiye

¹(sorumlu yazar), fcakici@yildiz.edu.tr , ORCID: 0000-0001-9752-1125

²rabia.yenilmez@std.yildiz.edu.tr, 0009-0004-3484-7258

ÖZET

Bu çalışmanın ilk amacı, geminin yalpa hareketinin sönümlenme karakterinin incelenmesidir. İkincisi ise sönüm parametresinin geminin ileri hızı, dalga frekansı ve başlangıç yalpa genliği açısının yalpa hareketi çözümündeki etkisini araştırmaktır. Yalpa hareketi, diğer serbestlik derecelerinden daha kritik ancak viskozite kaynaklı karmaşık doğasından dolayı en az anlaşılan bir harekettir. Yalpa sönümünün birkaç bileşeni vardır ve bunlar deneyler sonucunda oluşturulan ampirik formüller yardımıyla beş öğeye ayrılmıştır. Dalga sönümü, doğrusal difraksiyon/radyasyon teorisi ile hesaplanır, dolayısıyla doğrusal bir sönümdür. Kaldırma sönümü de doğrusal olarak kabul edilir. Bununla birlikte girdap oluşturma, sürtünme ve yalpa omurgası kaynaklı sönüm, başlangıç yalpa genliğine bağlı olduğundan doğrusal değildir. Bu çalışmada yalpa genliği, geminin ileri hızı ve dalga frekansının etkileri Ikeda ve Himeno tarafından geliştirilen ampirik formüllerle incelenmiştir. Önerilen makalenin güvenilirliğini göstermek için bazı senaryolarda yalpa hareketinin frekans düzlem analizleri de yapılmıştır. Tüm kodlamalar MATLAB kullanılarak yapılmıştır ve YTÜ DEEP Gemi Hareket Programına gömülecektir.

Anahtar kelimeler: Yalpa hareketi, Yalpa sönümü, Himeno metodu, YTU DEEP gemi hareket program

Makale geçmişi: Geliş 20/08/2023 – Kabul 20/11/2023

DOI: <https://doi.org/10.54926/gdt.1347001>

Comprehensive Roll Damping Assessment and Motion Analysis for a Benchmark Container Ship

Ferdi Çakıcı¹, Rabia Yenilmez²

^{1,2}Yıldız Technical University, Naval Architecture And Maritime Faculty, Department of Naval Architecture And Marine Engineering, İstanbul, Türkiye

¹(corresponding author), fcakici@yildiz.edu.tr , ORCID: 0000-0001-9752-1125

²rabia.yenilmez@std.yildiz.edu.tr, 0009-0004-3484-7258

ABSTRACT

The primary purpose of this study is to investigate the damping characteristics of the ship's roll motion. The second goal is to explore the damping effects on the solution of roll motion, considering the ship's forward speed, wave frequency, and initial roll amplitude. Roll motion is a more critical yet less understood response compared to other degrees of freedom due to the complexity arising from viscosity. Roll damping comprises several components, which are divided into five categories with the assistance of empirical formulas created as a result of experiments. Wave damping is calculated by linear diffraction/radiation theory so it is a linear damping. Lift damping is also considered linear. However, eddy making, skin friction, and bilge keel damping are not linear due to dependency on the initial roll amplitude. The effects of roll amplitude, the ship's forward speed, and wave frequency are investigated in this paper with the empirical formulas developed by Ikeda and Himeno. Frequency domain analyses of the roll motion are also conducted for the selected cases to demonstrate the credibility of the proposed paper. All algorithms have been developed in the MATLAB environment which is embedded with the YTU DEEP Ship Motion Program.

Keywords: Roll motion; Roll damping; Himeno's method; YTU DEEP ship motion algorithm.

Article history: Received 20/08/2023 – Accepted 20/11/2023

1. Introduction

Typically, a ship may undergo more rolling movement compared to other types of motion due to its narrower width relative to its length. Additionally, the roll experiences lower damping compared to other motions and its inertia is significantly smaller when compared to the other rotational motions. Roll motion may be considered the most critical response among the other motions according to recent literature. Its significance arises from the potential for large wave amplitudes, which can result in cargo shifting and, in some cases, capsizing. Accurately predicting roll damping is essential for ship stability, performance, and safety. However, unlike other degrees of freedom motion, roll damping and the restoring moment contain strong nonlinear components. The fluid damping in roll motion, also known as roll damping, holds an important role as it governs the magnitudes of wave-induced impacts. Accurately estimating the numerical values of roll damping presents a challenge due to its complex nature. While damping derived from diffraction and radiation theory suffices in defining surge, sway, heave, pitch, and yaw movements of the structure, it lacks adequacy in representing the modeling of roll damping. Roll damping is difficult to predict due to its nonlinear characteristics, arising from viscous effects. Furthermore, the characteristics of roll damping are influenced by factors such as the ship's forward speed, oscillation frequency, and initial roll angle.

Bilge Keels, the first designs of which were developed by William Froude (Sir A. Wescott, 1955), contributed to damping as passive stabilizers in roll motion. Following Froude's research on roll damping, the Japanese researchers have extensively studied ship roll damping and published several papers in which they predicted damping results. In the late 1970s, researchers such as Ikeda, Himeno, and Tanaka from Osaka Prefecture University in Japan published several studies. These studies not only summarized the findings of other researchers but also introduced a fundamentally novel and practical estimation technique for roll damping (Falzarano and Somayajula, 2015). According to their works, roll damping consisted of various components, including skin friction damping, eddy damping, bilge keel damping, lift damping, and wave damping. This sub-partitioning was introduced by these researchers and simplifies the estimation of numerical values. Each component contributed differently to the overall damping, and their interactions with roll damping were complex and complicated in terms of its prediction. Ikeda et al. (1978a) neglected the inter-component interaction and other degrees of freedom of roll. They also separated roll from other degrees of freedom. Ikeda et al. (1978b) also introduced a computer program developed to calculate the roll-damping coefficient, as described in an article published in Japanese language. However, some of the significant papers of them were translated into English by the Ikeda group (Falzarano and Somayajula, 2015).

Due to the detailed and comprehensive approach of the Japanese researchers, a substantial amount of work and experimentation has been conducted. Most of these experiments were implemented for 2-Dimensional shapes. The results of 3-dimensional shapes are currently under discussion (S. Chakrabarti, 2001). As a result of many experiments on the numerical values of the damping components, empirical formulas have been developed for estimations. Notably, Ikeda et al. have conducted comprehensive studies in this area. Schmitke (1978) investigated new methods to predict roll and also sway and yaw at about the same time as Japanese researchers and his method used some of the earlier their references. Himeno (1981) has analyzed roll damping through experimental investigations, focusing on the effects of different factors. This report contains computer programs to predict ship roll motion. The first computer program focuses on the ship and bilge keel, while the second program includes a more comprehensive component inspection approach. A large number of papers have been published and several computer programs have been released that fundamentally cited these comprehensive reports. For example, Chakrabarti (2001) and Falzarano and Somayajula

(2015) examined the damping components at zero speed and forward speed, taking references from Himeno (1981), Ikeda (1978a, 1978b) and Schmitke (1978).

The present paper aims to investigate roll damping by drawing references from Himeno (1981) and creating a computer program where roll damping becomes a function of wave frequency, initial roll angle, and the ship's forward speed. In the study of Olmez and Cakici (2022), they aimed to develop a ship motion program including roll motion calculation in waves but their calculations were limited because they used Ikeda's simplified code (Ikeda et al. (1978b) in which wave frequency and the ship's forward speed on roll damping are neglected. Therefore, the present report aims to contribute to the YTU DEEP ship motion program with a more accurate calculation of roll damping. In other expressions, the report aims to code the state-of-the-art empirical method of Himeno and examine the damping characteristics on the roll motion of a ship.

2. Mathematical Model for Roll Motion

The roll motion equation, which mathematically describes the ship's roll motion, contains external effects and stability considerations. Based on Newton's second law, this equation consists of roll moment, inertia, and damping. The roll motion equation is expressed in a single degree of differential equation, unlike other degrees of motion of ships, barges, and semisubmersibles, and cannot be well defined linearly because of nonlinear damping and restoring. The equation of motion in a roll may be expressed as:

$$I\ddot{\varphi} + B(\dot{\varphi}) + C(\varphi) = M\cos(\omega t) \quad (1)$$

Here, φ is defined as angular roll motion, dots represent time derivatives, I is the total moment of inertia in roll, M is the wave exciting moment, ω is the wave frequency and t is time. The damping coefficient, B , and the restoring coefficient, C are nonlinear coefficients. The nonlinearity is expressed as a polynomial. The damping term, B may be expressed by:

$$B(\dot{\varphi}) = B_1\dot{\varphi} + B_3\dot{\varphi}^3 \quad (2)$$

Where the first term, damping is linear in Equation 2, the second term is expressed as quadratic damping and the third term is cubic damping. Total damping is roughly estimated as an equivalent linear damping:

$$B(\dot{\varphi}) = B_{eq}\dot{\varphi} \quad (3)$$

The roll equation is linearized with the nonlinear term obtained by applying the Fourier transform (Himeno (1981)). B_{eq} is described as an equivalent damping coefficient. Nonlinear coefficients are shown as:

$$B_{eq} = B_1 + \frac{3}{4}B_3(\omega R_0)^2 \quad (4)$$

where R_0 is the amplitude of roll motion and ω is the wave frequency. The empirical method gives B_{eq} . This equivalent damping is the function of the initial roll angle. Therefore, to obtain B_1 and B_3 given in

equation 2, a simple mathematical trick should be applied as suggested by the related IMO (2016) document. This procedure is also given at the beginning of Section 5.

3. Roll Damping Formulation

The components that contribute to roll damping are expressed below (Himeno, 1981). Total equivalent damping is the sum of the following components:

$$B_{eq} = B_F + B_E + B_W + B_L + B_{BK} \quad (5)$$

in which B_F : hull skin friction damping, B_E : hull eddy shedding damping, B_W : free surface wave damping, B_L : lift damping, and B_{BK} : bilge keel damping.

3.1 Skin Friction

When the ship moves, the friction force that occurs on the surfaces in contact with the water slows the ship's movement and causes energy loss. Skin friction damping creates a resistance to roll motion. It depends on the wetted surface area, the frequency of the wave, the viscosity of the water, the amplitude of the roll motion, and the effective bilge keel radius. For zero speed ($U=0$) in a laminar flow field, Kato (1965) gives the friction coefficient as:

$$B_{f0} = \frac{4}{3\pi} \rho S r_e^3 R_0 \omega C_f \quad (6)$$

in which the friction coefficient C_f is given by:

$$C_f = 1.328 \left[\frac{2\pi\nu}{3.22r_e^2 R_0^2 \omega} \right]^{\frac{1}{2}} \quad (7)$$

The effective bilge radius is computed from:

$$r_e = \frac{1}{\pi} \left[(0.887 + 0.145C_B) \frac{S}{L} - 2OG \right] \quad (8)$$

where ρ : water density, ν : kinematic viscosity of water, ω : wave frequency, B : beam, D : draft, L : lateral dimension of the ship, CB : block coefficient of the ship, R_0 : the amplitude of roll motion (in radians), and U : forward speed (or steady current speed). OG is the vertical distance from the origin O (still water level) to the roll axis, G , which is measured positively downward ($OG=D-KG$). The ship's wetted surface area, S is calculated approximately as:

$$S = L(1.7D + C_B B) \quad (9)$$

$$Re = \frac{\rho VL}{\mu} \quad (10)$$

It should be noted that the skin friction coefficient is a function of the Reynolds number.

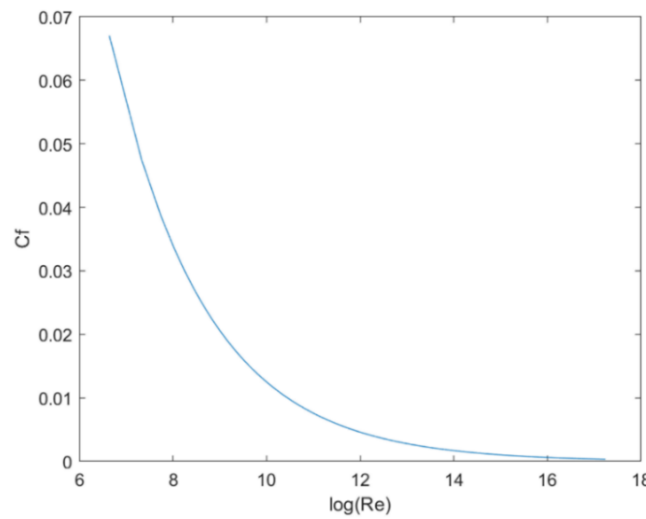


Figure 1. Skin friction vs. Reynolds number

As seen in Figure 1, skin friction vs. Reynolds number relate to each other. The presence of an effective bilge keel radius changes the value of skin friction. In addition, as the speed of the ship increases, more friction force will be created, so skin friction damping also changes. Since ship models are small-scale, they are experienced by laminar flow. Full-scale ships are affected by a turbulent flow due to the high Reynolds number. Therefore, an arrangement for turbulent flow is required. The equation in which turbulent flow is taken into account is as follows:

$$B_{f0} = 0.787\rho S r_e^2 \sqrt{\omega\nu} \left\{ 1 + 0.00814 \left(\frac{r_e^2 R_0^2 \omega}{\nu} \right)^{0.386} \right\} \quad (11)$$

The first term of the above expression is linear and is independent of roll amplitude. The second term indicates that the skin friction damping of the ship in turbulent flow is nonlinear. It is noted that the roll angle might change from 0° to 20°. Skin friction gradually and consistently increases as the roll angle changes. It is also expected to change in the non-zero Froude number:

$$F_n = U/\sqrt{gL} \quad (12)$$

Where g is the gravitational acceleration. U, Schmitke (1978) merged the relationship between the above formula and speed for non-zero forward speed:

$$B_f = B_{f0} \left(1 + 4.1 \frac{U}{\omega L} \right) \quad (13)$$

The coefficient 4.1 given in Equation 13 was found as a result of experiments with a spheroid object. During the experiments, data were collected by measuring the speed, direction of movement, and other parameters of the spheroid. Furthermore, skin friction damping estimates were made by computational methods. It is shown that skin friction increases slightly with the contribution of speed in the formulation. For ships, this formula can be used in case of currents or waves. While the results are expected to increase due to the scale effect, this formula is applicable for a full-scale ship as the contribution of skin friction to damping is very small. Figure 2 shows BFO vs. initial roll amplitude.

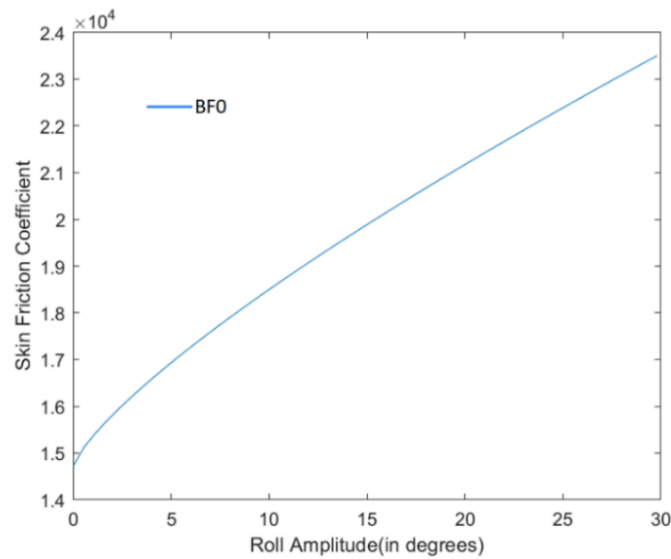


Figure 2. Roll Amplitude and Skin Friction Coefficient Graph

Remark 1. In the new version of the YTU DEEP Ship motion program, Equation 11 and Equation 13 will be used for the skin friction-damping component. On the other hand, In the old version of the YTU DEEP Ship motion program Equation 6 was used for skin friction damping component and the effects of the forward speed are ignored.

3.2 Eddy Making

Eddy making is the damping component caused by the eddies that form around the ship during its circular roll motion. An eddy refers to the rotational motion arising due to the fluid's movement while in motion. Especially in high-velocity flows or in sections of the ship near the bow, stern and in areas such as those close to the bilge keel, eddies form, causing a disturbance in the flow. The interaction between eddies and waves emerges due to the ship's forward speed, resulting in energy loss and a decrease in the ship's forward speed. In this study, Ikeda's Formulas are used for the calculation. Equivalent to this formulation:

$$C_p = 0.5[0.87 \exp(-\gamma) - 4 \exp(-0.187\gamma) + 3] \quad (14)$$

The velocity increment ratio:

$$\gamma = \frac{\sqrt{\pi f_3}}{2[D - OG]\sqrt{H_0'\sigma'}} \left[r_{max} + \frac{2M}{H_1} \sqrt{A_1^2 + B_1^2} \right] \quad (15)$$

where:

$$H_1 = 1 + a_1^2 + 9a_3^2 + 2a_1(1 - 3a_3) \cos 2\psi - 6a_3 \cos 4\psi \quad (16)$$

$$A_1 = -2a_3 \cos 5\psi + a_1(1 - a_3) \cos 3\psi - \{(6 - 3a_1)a_3^2 + a_1(a_1 - 3)a_3 + a_1^2\} \cos \psi \quad (17)$$

$$B_1 = -2a_3 \sin 5\psi + a_1(1 - a_3) \sin 3\psi - \{(6 + 3a_1)a_3^2 + a_1(a_1 + 3)a_2 + a_1^2\} \sin \psi \quad (18)$$

$$M = \frac{B}{2(1 + a_1 + a_3)} \quad (19)$$

and

$$C_R = \left[\frac{r_{max}}{D} \right]^2 \left[1 - f_1 \frac{R_b}{D} \right] \left[1 - \frac{OG}{D} - f_1 \frac{R_b}{D} \right] + f_2 \left[H_0 - f_1 \frac{R_b}{D} \right]^2 \quad (20)$$

in which C_R is computed at incremental ship station. The quantities R_b : bilge radius, OG : distance (positive downward) from O to G , H_0 : half the beam-draft ratio at different stations of the ship (a variable depending on the shape of the ship):

$$\sigma = \frac{A_x}{B_x D_x} \quad (21)$$

$$0.9 \leq \sigma \leq 1.0$$

$$H_0 = \frac{B}{2D} \quad (22)$$

and

$$H'_0 = \frac{H_0 D}{D - OG} \quad (23)$$

and

$$\sigma' = \frac{\sigma D - OG}{D - OG} \quad (24)$$

and

$$R_b = 2d \sqrt{\frac{H_0(\sigma - 1)}{\pi - 4}} \quad \text{for } R < D, R < B/2 \quad (25)$$

$$R_b = D \quad \text{for } H_0 \geq 1, R/D > B/2 \quad (26)$$

$$R_b = B/2 \quad \text{for } H_0 < 1, R/D > H_0 \quad (27)$$

where s : area coefficient at a cross-section along the hull ($\sigma_x = \text{area}/(B_x D_x)$).

The terms f_1 , f_2 and f_3 are as follows:

$$f_1 = 0.5[1 + \tanh\{20(\sigma - 0.7)\}] \quad (28)$$

$$f_2 = 0.5[1 - \cos \pi \sigma] - 1.5[1 - \exp\{-5(1 - \sigma)\}] \sin^2 \pi \sigma \quad (29)$$

$$f_3 = 1 + 4 \exp\{-1.65 \times 10^5 (1 - \sigma)^2\} \quad (30)$$

$$r_{max} = M[\{(1 + a_1)\sin\psi - a_3 \sin 3\psi\}^2 + \{(1 - a_1)\cos\psi + a_3 \cos 3\psi\}^2]^{1/2} \quad (31)$$

$$\psi = \frac{1}{2} \cos^{-1} \frac{a_1(1 + a_3)}{4a_3} \quad (32)$$

a_1 and a_3 are Lewis form constants corresponding to the shape of the cylinder. For a 3-dimensional ship, the above coefficients are integrated with the length of the ship. The above formulation has been modified by Ikeda (1984) as there will be variations in the numerical result of the effect of sharp corners on a barge. Since the corners are sharp, they are independent of the bilge radius:

$$B_{e0} = \frac{2}{\pi} \rho L D^4 (H_0^2 + 1 - OG/D) [H_0^2 + (1 - OG/D)^2] R_0 \omega \quad (33)$$

The barge with sharp corners is more suitable for this formula. However, it is noteworthy that the formulation is a linear function of roll amplitude and wave frequency. Ikeda et al. (1978a,b) combined a coefficient that is a function of forward speed with the eddy-making damping coefficient:

$$B_e = B_{e0} \left[\frac{(0.04\omega L/U)^2}{1 + (0.04\omega L/U)^2} \right] \quad (34)$$

Ikeda et al. (1978a, b) combined a coefficient that is a function of forward speed with the eddy-making damping coefficient. It should be noted that the eddy-making damping coefficient decreases in the presence of forward speed.

Remark 2. It is very important to underline that the all formulations explained above are only valid for σ greater than 0.90. Therefore, the calculations are done for the mid-ship section and then integrated over the length of the ship in the new version of the YTU DEEP Ship motion program.

Remark 3. In some papers in the literature (for example, Chakrabarti (2001)), a_1 and a_3 coefficients were defined as roll decay extinction coefficients due to the lack of information in Himeno's original Japanese report (1981). However, as Falzarano and Somayajula (2015) underlined, these coefficients come from the geometry of the hull with the implementation of conformal mapping.

3.3. Lift Damping

Lifting damping occurs as a result of a lifting moment similar to the lift force in the forward speed movement of the ship. Ikeda et al. (1978 a,b) lifting damping explained as:

$$B_L = \frac{0.15}{2} \rho U L D^3 k_N \left[1 - 2.8 \frac{OG}{D} + 4.667 \left(\frac{OG}{D} \right)^2 \right] \quad (35)$$

where the slope constant of the lift coefficient:

$$k_N = 2\pi \frac{D}{L} + \kappa \left(4.1 \frac{B}{L} - 0.045 \right) \quad (36)$$

and

$$\kappa = 0, \quad \text{for } \sigma < \sigma = 0.92 \quad (37)$$

$$\kappa = 0.1, \quad \text{for } 0.92 < \sigma < \sigma = 0.97 \quad (38)$$

$$\kappa = 0.3, \quad \text{for } 0.97 < \sigma < \sigma = 0.99 \quad (39)$$

It is noteworthy that the lift damping is linear. σ is the midsection coefficient. In the case of zero speed ($U=0$), lift damping will not occur. Lift damping is independent of the frequency of the wave. The most important part is that the contribution of the lift to the total damping is very high with forward speed increase.

3.4. Wave Damping

Wave damping, a function of wave parameters, results from free surface waves. The diffraction/radiation theory is used to examine the hydrodynamic behavior of the ship under the influence of waves. Thus, the wave forces and interaction with the wave surface of the ship are calculated. It is commonly known as radiation-damping B_{w0} . Wave damping is a function of forward velocity and wave frequency. The presence of forward velocity changes wave damping. A formulation for damping has been derived for a plate by introducing a pair of dummies at the two longitudinal ends (Ikeda et al., 1978a). Wave attenuation at forward velocity is shown as:

$$B_w = B_{w0} \frac{1}{2} \{ [(A_2 + 1) + (A_2 - 1) \tanh(20(\tau - 0.3))] + (2A_1 - A_2 - 1) \exp(-150(\tau - 0.25)^2) \} \quad (40)$$

and

$$A_1 = 1 + \xi_d^{-1.2} \exp(-2\xi_d) \quad (41)$$

$$A_2 = 0.5 + \xi_d^{-1.0} \exp(-2\xi_d) \quad (42)$$

$$\xi_d = \omega^2 d / g \quad (43)$$

$$\tau = U\omega / g \quad (44)$$

B_{w0} is calculated according to diffraction theory and its formulation is well published in the simplified Ikeda's code (Ikeda, 1978b). It should be considered that the damping coefficient is maximum at $\tau=1/4$ and approaches a constant value at large values. This equation can be applied to ships under the effect of slow drift motion with high frequency.

Remark 4. In the old version of the YTU DEEP Ship motion program, B_{w0} was used for wave damping. In the new version of the YTU DEEP Ship motion program, B_w is used that way the forward speed effects on wave damping are added.

3.5. Bilge-keel Damping

Bilge keels generate dynamic interactions on contact with the free surface. Thanks to these interactions, damping occurs, which is a soothing force. Bilge keels are the most efficient way to increase damping, thereby reducing the ship's roll motion (Boston, 1972). In this way, the ship becomes more stable. The bilge keel on the ship consists of a normal force on the keel and the pressure variations on the hull surface caused by the bilge keel. These components show the effects of bilge keels between the hull surface and the waves.

The new expression, which is derived from experiments, was published by Ikeda et al (1978a). In addition, the effect of the wave is neglected. The new expression, which is obtained by the effects of normal force and pressure force, is shown as:

$$B_{BK} = B_{BKN} + B_{BKH} \quad (45)$$

The normal force component per unit length is written as:

$$B_{BKN} = \frac{8}{3\pi} \rho r_{cb}^3 b_{BK} \omega R_0 f^2 C_D \quad (46)$$

In terms of an equivalent drag coefficient:

$$C_D = 22.5 \frac{b_{BK}}{\pi r_{cb} R_0 f} + 2.4 \quad (47)$$

where b_{BK} : is the width of the bilge keel and f is the correction factor for the bilge keel, considering the increase in flow speed:

$$f = 1 + 0.3 \exp\{-160(1 - \sigma)\} \quad (48)$$

The expression is obtained by the pressure measurement due to the presence of Bilge Keel as follows:

$$B_{BKH} = \frac{4}{3\pi} \rho r_{cb}^2 D^2 \omega R_0 f^2 \left\{ - \left(-22.5 \frac{b_{BK}}{\pi r_{cb} R_0 f} - 1.2 \right) A_2 + 1.2 B_2 \right\} \quad (49)$$

where:

$$A_2 = (m_3 + m_4)m_8 - m_7^2 \quad (50)$$

$$B_2 = \frac{m_4^3}{3(H_0 - 0.215m_1)} + \frac{(1 - m_1)^2(2m_3 - m_2)}{6(1 - 0.215m_1)} + (m_3m_5 + m_4m_6)m_1 \quad (51)$$

$$m_1 = \frac{R_b}{D}; \quad m_2 = \frac{OG}{D}; \quad m_3 = 1 - m_1 - m_2; \quad m_4 = H_0 - m_1 \quad (52)$$

$$m_5 = \frac{0.414H_0 + 0.0651m_1^2 - (0.382H_0 + 0.0106)m_1}{(H_0 - 0.215m_1)(1 - 0.215m_1)} \quad (53)$$

$$m_6 = \frac{0.414H_0 + 0.0651m_1^2 - (0.382 + 0.0106H_0)m_1}{(H_0 - 0.215m_1)(1 - 0.215m_1)} \quad (54)$$

$$m_7 = S_0/D - 0.25\pi m_1 \quad \text{for } S_0 > 0.25\pi R_b \quad (55)$$

$$m_7 = 0 \quad \text{otherwise} \quad (56)$$

$$m_8 = m_7 + 0.414m_1 \quad \text{for } S_0 > 0.25\pi R_b \quad (57)$$

where

$$S_0 = 0.3\pi f r_{cb} R_0 + 1.95b_{BK} \quad (58)$$

The bilge-circle radius, R_b and the mean distance, r_{cb} from the roll axis to the bilge keel is given by:

$$R_b = 2D \sqrt{\frac{H_0(\sigma - 1)}{\pi - 4}} \quad \text{for } R_b < D, R_b < B/2 \quad (59)$$

$$R_b = D \quad \text{for } H_0 \geq 1, R/D > 1 \quad (60)$$

$$R_b = B/2 \quad \text{for } H_0 \leq 1, R/D > H_0 \quad (61)$$

$$r_{cb} = D \left[\left\{ H_0 - \frac{0.293R_b}{D} \right\}^2 + \left\{ 1 - \frac{OG}{D} - \frac{0.293R_b}{D} \right\}^2 \right]^{\frac{1}{2}} \quad (62)$$

Remark 5. B_{BKN} and B_{BKH} are calculated for the midship section. In order to obtain the overall bilge keel damping, this value should be multiplied by the bilge keel length.

4. Damping Evaluation for a Container Ship

The coding including the above formulations has been implemented and the evaluation of damping is obtained for a container ship's form in this report. The parameters of the sample vessel with bilge keel (a container ship) are given in Table 1.

Table 1. Parameters of sample container ship

L	262 m
B	40 m
T	12 m
C_b	0.576
Δ	73,348 t
GMt	2.8 m
LBK	72 m
BBK	0.4 m
KG	17.51 m
$\sigma (C_M)$	0.957

In Table 1, L is the length between perpendiculars, B is the moulded breath, T is the moulded draught, C_B is the block coefficient, Δ is the weight, GMt is the transversal metacenter height, KG is the vertical center of gravity and finally σ is midship area coefficient of the ship. LBK is the bilge keel length, and BBK is the bilge keel breath. 2D sections of the sample container ship are given in Figure 3.

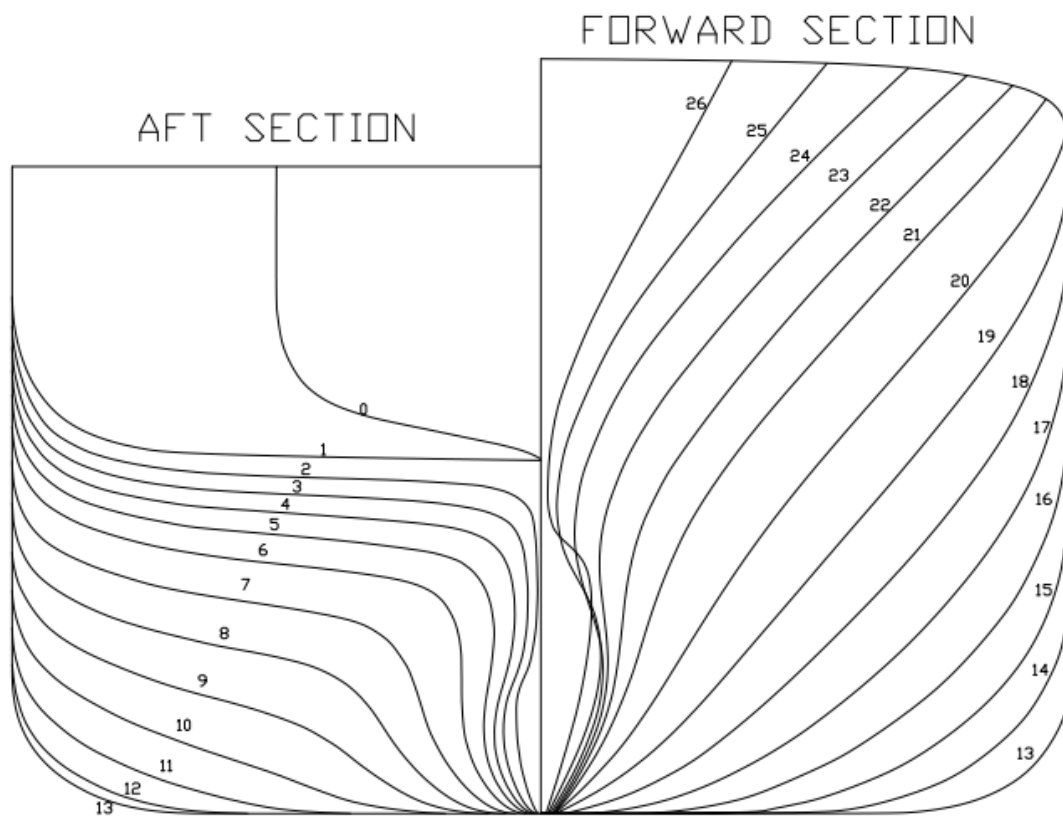


Figure 3. 2D Sections of the Sample Container Ship

The results of the studies were evaluated on the sample vessel. It is underlined that the roll damping might remarkably depend on the initial roll angle, the wave frequency, and the forward speed of the ship. Therefore, the portion of these three effects could be very important considering the investigated case. For example, the damping characteristics at low wave frequencies differ from the characteristics at high frequencies. In the same way, zero forward speed and non-zero forward speed conditions would be quite different when evaluating the roll damping. Therefore, the properties of the ship's forward speed, wave frequency, and roll amplitude would directly affect the roll motion characteristics. The coefficients in these empirical formulas (Himeno, 1981), which depend on the ship's form, were obtained. These formulas are coded using a MATLAB program.

The sum of the linear and nonlinear components gives equivalent damping. The sum of these components has been studied at different initial roll amplitudes and ship's forward speeds. Figure 4 shows the B_{eq} vs. wave frequency with different proportions of damping components at different ship speeds and initial roll angles.

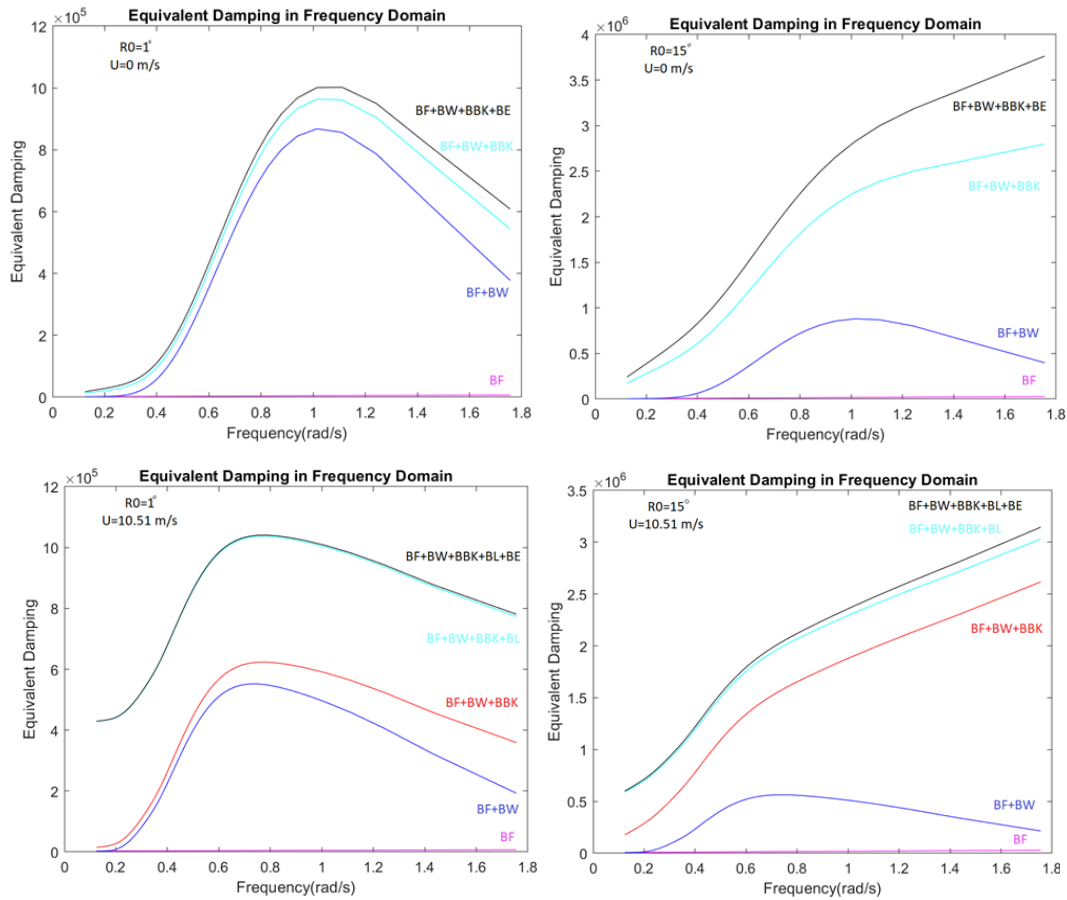


Figure 4. Equivalent Damping vs Wave Frequency

Based on the graphs, the following conclusions can be reached; In cases where the speed is zero, it has been observed that the lift damping is zero, but the other components have low or high contributions. In addition, one can observe that equivalent damping increases as the roll amplitude increases for these cases.

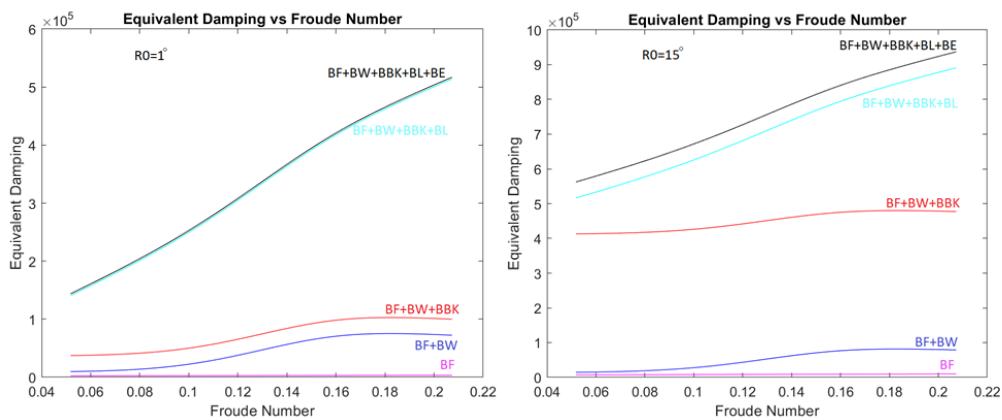


Figure 5. Equivalent Damping vs Froude Number

The result obtained from Figure 5, the equivalent damping graphs examined according to the speed (Froude Number) is as follows; as the initial roll angle and the forward speed increase, the equivalent damping increases. It is noted that the natural frequency is considered in Figure 5.

4.1 Evaluation of Effect With and Without Bilge Keel

In this section, the effect of the presence of bilge keels on damping is examined.

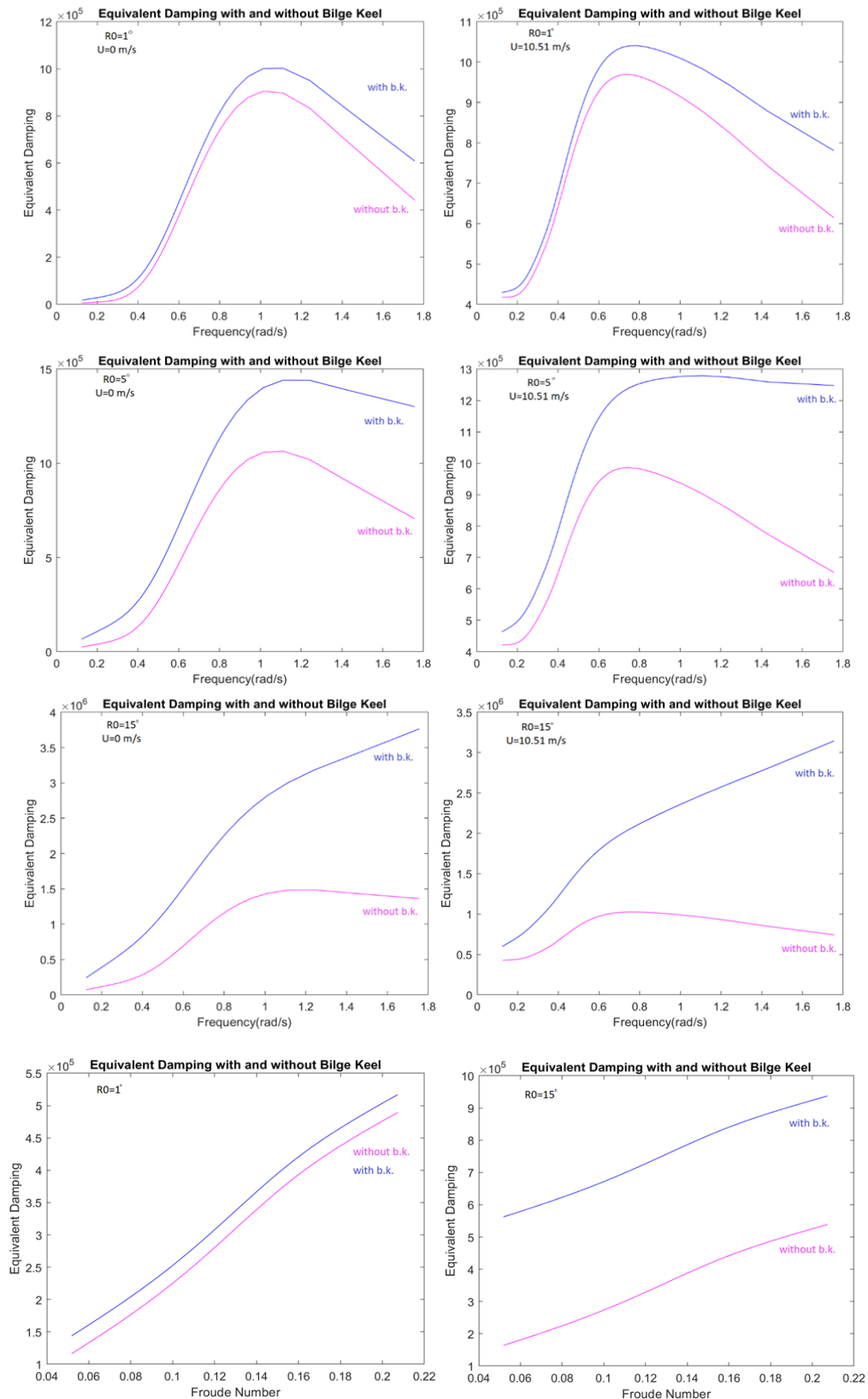


Figure 6. Equivalent Damping with/without bilge keel

Observing the graphs above shows that the presence of the bilge keel makes a significant contribution to the damping in the case of zero forward speed ($U=0$). In addition, it has been observed that the increase in Roll Amplitude at $U=0$ contributes to almost three times the equivalent damping of the bilge keels. The presence of bilge keel was also investigated with the increase of speed and roll amplitude, and it was observed that equivalent damping increased as roll amplitude increased. However, it should be taken into account that some components decrease as the forward speed increases, so how much the bilge keel contributes to equivalent damping cannot be obtained from these graphs. From the graphs given in Figure 6, one can observe that the increase in speed at the ship's natural frequency, coupled with the presence of a bilge keel, leads to an increase in equivalent damping.

4.2 Evaluation of Effect of Forward Speed on Roll Damping

The responses of the components to the ship's forward speed change are different. For example, in different cases, damping may even decrease as forward speed increases. As the roll amplitude increases, the ship's damping at zero speed is examined in Figure 7. At very low initial roll angles, damping increases at most frequencies as the forward speed increases.

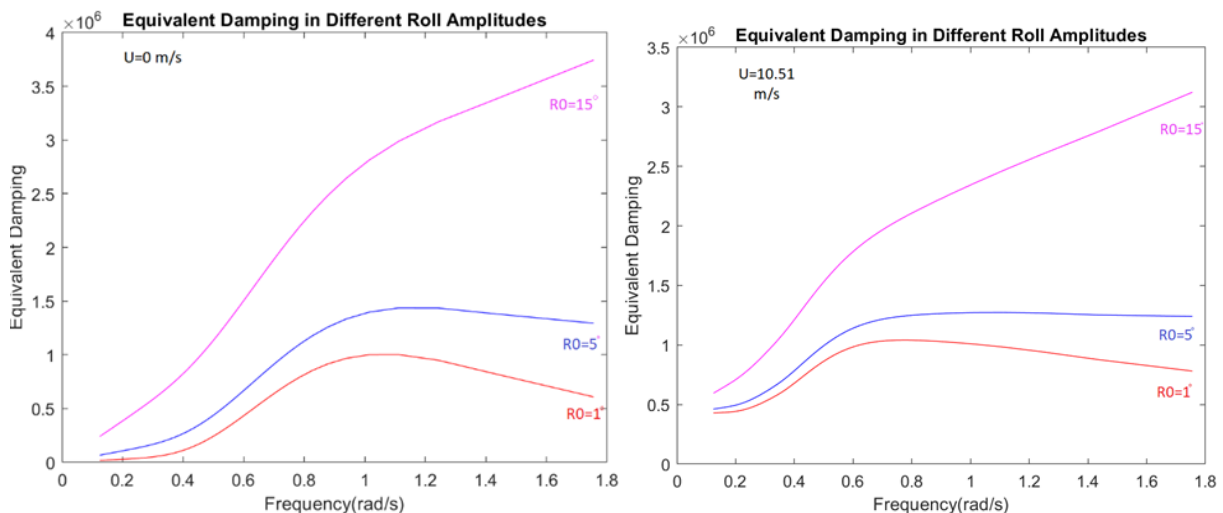


Figure 7. Equivalent Damping in Different Forward Speeds with Different Amplitudes

4.3 Evaluation of Effects Initial Roll Amplitudes

The change in the initial roll amplitude also affects the equivalent damping. As can be seen from Figure 8, increasing the forward speed also increased the damping at low frequencies, and increasing the initial roll angle increased the damping at the entire frequency region.

5. Frequency Domain Roll Motion Calculations

For Frequency Domain analyses, linear damping is calculated. Himeno's empirical method gives the equivalent damping and it is the function of the initial roll angle. Therefore, to obtain B_1 and B_3 separately, a simple mathematical assumption is applied as suggested by the related the annex in IMO document (2016). The details are given in Section 5.1.

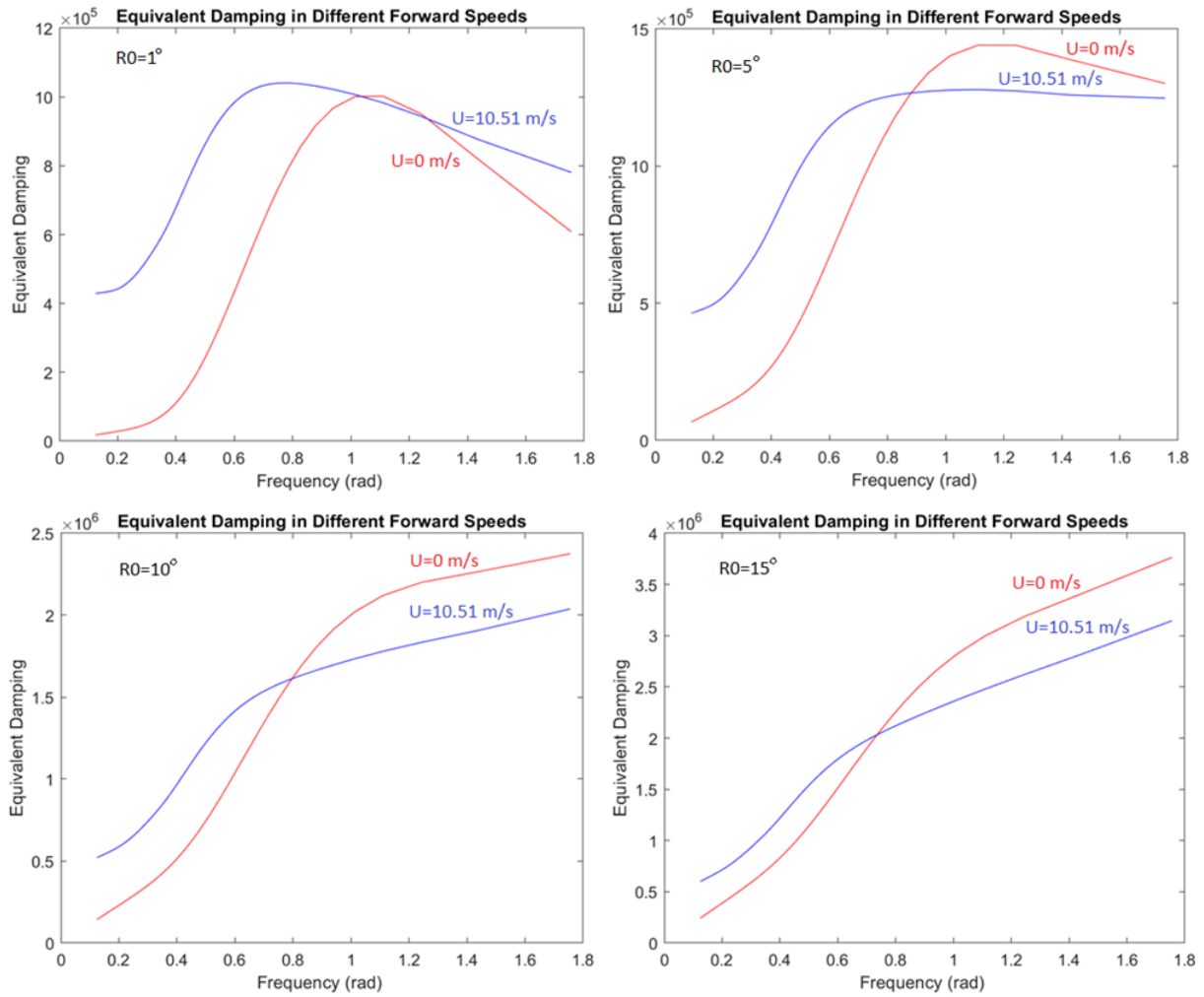


Figure 8. Equivalent Damping for different Initial Roll Amplitudes

5.1 Linear and Cubic Coefficient

The roll motion in calm water can be modeled as follows:

$$I\ddot{\varphi} + B(\varphi) + C(\varphi) = 0 \quad (63)$$

where the right-hand side vector is zero since it is calm water.

If the equivalent linear damping coefficient is introduced instead of nonlinear B, and linear restoring is used, the following equation is obtained:

$$I\ddot{\varphi} + B_{eq}\dot{\varphi} + \Delta gGMt\varphi = 0 \quad (64)$$

then,

$$\ddot{\varphi} + 2\alpha + \omega_{\varphi}^2\varphi = 0 \quad (65)$$

where:

$$2\alpha = \frac{B_{eq}}{I}$$

$$\omega_\varphi = \sqrt{\frac{\Delta g GM t}{I}}$$

On the other hand, the solution of equation (63) is given by and the extinction curve is given by:

$$\varphi = \varphi_0 e^{-\alpha t} \cos(\omega_\varphi t - \varepsilon)$$

and the extinction curve is given by:

$$\Delta\varphi = a\varphi_m + c\varphi_m^3 = (a + c\varphi_m^2)\varphi_m \quad (66)$$

where:

$\Delta\varphi$: decrement of roll decay tests (radians); and

φ_m : mean swing angle of roll decay test (radians).

Thus,

$$a_e = \frac{\alpha T_\varphi}{2} = \frac{\alpha\pi}{\omega_\varphi} = \frac{B_{eq}}{2I} \frac{\pi}{\omega_\varphi} \quad (67)$$

Using the above relationship, a procedure to determine linear and cubic damping coefficients is as follows:

1. First, B_{eq} is obtained with the roll amplitude, φ_a , of 1 degree using Himeno's method. Using equation (67) and assuming $a = a_e$, the value of a is obtained
2. Then, B_{eq} is obtained with the roll amplitude of 25 degrees using Ikeda's simplified method. Using equation (67), the value a_e is obtained.
3. Then, c is determined with the following equation, and the value of a determined in step 1:

$$a_e = (a + c\varphi_m^2) \quad (68)$$

where φ_m corresponds to 25 degrees.

4. Using the well-known energy relationship, linear and cubic roll damping coefficients can be calculated as follows:

$$\alpha = \frac{\omega_\varphi}{\pi} a \quad (69)$$

$$\gamma = \frac{4c}{3\pi^2} \frac{2\pi}{\omega_\varphi} \quad (70)$$

Noted that $B_1 = 2\alpha I$ and $B_3 = \gamma I$.

5.2 Low Steepness Approximation

The low slope approximation is generally used for roll motion calculations in regular waves. According to this approach, the wavelength by putting the ship into roll motion is considerably larger than the beam of the ship. so the frequency is assumed very small.

The roll motion equation in the time domain is given:

$$(I_{44} + A_{44})\ddot{\varphi}(t) + B_1\dot{\varphi}(t) + C_{44}\varphi(t) = M(t) \quad (71)$$

To solve this equation in the frequency domain:

$$\varphi(t) = \{Re\}|\varphi|e^{i\omega t + \beta t}$$

$$\dot{\varphi}(t) = i\omega\{Re\}|\varphi|e^{i\omega t + \beta t}$$

$$\ddot{\varphi}(t) = -\omega^2\{Re\}|\varphi|e^{i\omega t + \beta t}$$

$$M(t) = |M|e^{i\omega t + \beta t}$$

β is the phase angle between the roll moment peak point and wave profile in the center of gravity, and $\beta\eta$ shows the phase angle between the roll motion peak point and wave profile in the center of gravity:

$$(I_{44} + A_{44}) - \omega^2\{Re\}|\varphi|e^{i\omega t + \beta t} + B_1i\omega\{Re\}|\varphi|e^{i\omega t + \beta t} + C_{44}\{Re\}|\varphi|e^{i\omega t + \beta t} = |M|e^{i\omega t + \beta t}$$

In this condition, ω goes to zero, therefore simplified equation can be written as:

$$C_{44}|\varphi|e^{i\omega t + \beta t} = |M|e^{i\omega t + \beta t}$$

The ship follows the linear motion wave amplitude. The roll motion occurs at the slope of the wave:

$$\beta = \beta_\eta, |\varphi| = Ak_\eta, \text{ and } C_{44}Ak_\eta = |M|$$

A is the wave amplitude and k_η is the wave number. The inertia moment of roll motion, I_{44} , is expressed as:

$$I_{44} = \Delta k_{xx}^2 \text{ and } 0.35B < k_{xx} < 0.40B$$

where k_{xx} is the gyration radius for roll motion. The global added mass A_{44} and the hydrostatic restoring C_{44} coefficients for the roll motion are calculated as follows:

$$A_{44} = 0.30I_{44} \text{ and } C_{44} = g\Delta GM_t$$

where g is the gravity constant.

Frequency domain calculation in roll damping means analyzing roll motion in the frequency domain. Roll damping is studied at different frequencies to understand its properties and responses. In roll motion, how the ship responds to waves of different frequencies is measured by a function. This

function is the RAO (Response Amplitude Operator) graph. It represents the transfer function between the applied wave slope and the resulting response of the ship. RAO is considered a function of frequency that explains how the ship, which is exposed to different forces at different frequencies, will respond to roll motion. RAO values provide information about a ship's natural roll frequency, damping, and resonance behavior.

$$[A][z] = F \quad (72)$$

$[A]$ represents the coefficient matrix in the frequency domain. $[z]$ is the matrix expressing the response motions of the roll. $[F]$ is the matrix containing the excitation terms for the regular wave. The expressions in the $[F]$ matrix are created by using low steepness wave approximation for roll motion. Note that B_1 is the function of wave frequency. ω_e is encounter frequency and it is a function of wave frequency, ship speed and route.

$$A = \begin{bmatrix} -(I_{44} + A_{44})\omega_e^2 + C_{44} & -B_1(\omega_e)\omega_e \\ B_1(\omega_e)\omega_e & -(I_{44} + A_{44})\omega_e^2 + C_{44} \end{bmatrix}$$

$$F = \begin{bmatrix} \{Re\}M \\ \{Im\}M \end{bmatrix}$$

$$z = \begin{bmatrix} \{Re\}\varphi \\ \{Im\}\varphi \end{bmatrix}$$

$$z = (A)^{-1}F$$

$$z_4 = \sqrt{(\{Re\}\varphi)^2 + (\{Im\}\varphi)^2}$$

$$Roll\ RAO = \frac{z_4}{k_\eta A}$$

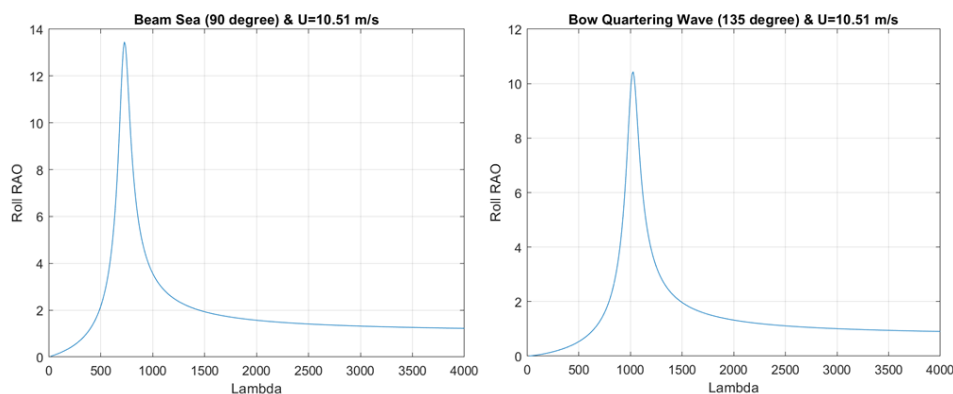


Figure 9. RAO Graph for Beam and Bow Quartering Wave in $U=10.51$ m/s

By the solution of Equation (72) for different routes, Figure 9 is obtained. It is noted that Λ denotes the wavelength in Figure 9 and is computed as:

$$\Lambda = \frac{2\pi g}{\omega^2}$$

6. Conclusions

Based on the available data, various components have been identified as influential in the damping of a ship's roll motion. There are five primary components used to calculate the total damping. Therefore, experimental formulas have been developed to calculate the damping contributions of skin friction, eddy, lift, wave, and bilge keel. The *Skin friction*, which has a non-linear equation, is dependent of roll amplitude and emerges as a component dependent on the vessel's speed. On the other hand, *Eddy damping* has been observed to increase with an increase in roll amplitude under the same speed conditions, and, in this context, the forward speed of the vessel is of significant importance. The linear component, *Lift damping*, does not contribute to total damping when the velocity component is zero, but it generates a substantial damping force as the speed increases. *Wave damping*, calculated based on diffraction/radiation theory, is a component that, while not directly related to roll amplitude, creates damping forces that increase with higher speeds, even though with smaller contributions compared to other components. Especially in situations where the roll amplitude increases, *Bilge keel* has been observed to make a significant contribution to the total damping, providing up to 52% of the total damping. It is believed that these empirical formulas can also be applied to 3D vessels, although these formulas are based on the results of 2D model experiments. These experiments were conducted on a small scale, and it is expected that there may be a scale effect on the results.

As a result, the effects of roll amplitude, speed, and bilge keel on damping have been thoroughly examined. It is not possible to calculate the roll damping theoretically. Therefore, empirical formulas are still the most powerful estimation technique for roll damping. This paper aimed to develop the YTU DEEP ship motion program by adding the most detailed empirical approach that regarded the effects of the initial roll angle, the ship's forward speed, and wave frequency. A containership has been taken to show the outputs of the coding. Results showed that the increase in the initial roll amplitude at very low speeds has also increased the total damping, especially near to the natural frequency. According to simulation results, the increase in the forward speed of the ship and the increase in the initial roll amplitude in the low-frequency region caused the total damping to increase. Furthermore, the contribution rate of the bilge keel to the total damping varies based on the ship's speed and roll amplitude.

Acknowledgements

This study is supported by project number 123M482 of the Scientific and Technological Research Council of Türkiye.

References

- Sir Wescott, A., (1955). The papers of William Froude M.A., LL.D, F.R.S., A Memoir. The Institution of Naval Architects, 11-13.
- Ikeda, Y., Himeno, Y., Tanaka, N., (1978a). Components of roll damping of ship at forward speed. Report No.00404, Department of Naval Architecture, University of Osaka Prefecture, Osaka, Japan.
- Ikeda, Y., Himeno, Y., Tanaka, N., (1978b). A prediction method for ship roll damping. Report No. 00405, Department of Naval Architecture, University of Osaka Prefecture, Osaka, Japan.
- Chakrabarti, S., (2001). Empirical calculation of roll damping for ships and barges. Ocean Engineering, 28, 915–932.

Himeno, Y., (1981). Prediction of ship roll damping state of the art., Report No. 239, Department of Naval Architecture and Marine Engineering, The University of Michigan, Ann Arbor, MI. September

Schmitke, R.T., (1978). Ship Sway, Roll, and Yaw Motions in Oblique Seas. Transactions Society of Naval Arch and Marine Eng., 86.

Kato, H., (1965). Effects of bilge keels on the rolling of ships. J. Society of Naval Architecture of Japan 117(in Japanese).

Falzarano, J.M, Somayajula, A. (2015). An Overview of the Prediction Methods for Roll Damping of Ships, Ocean Systems Engineering, 5, 55-76, DOI: 10.12989/ose.2015.5.2.055.

Olmez A., Cakici F., (2022). Theoretical manual of 'YTU DEEP' Ship motion program, 266,112451, Doi: 10.1016/j.oceaneng.2022.112451.

Submitted by Japan and Report of correspondence group part 2, IMO document (2016). Finalization Of Second Generation Intact Stability Criteria, SDC 4/5/1/Add.1 Annex 2, page 18.